Eur. Phys. J. E (2009)
DOI 10.1140/epje/i2009-10498-2

THE EUROPEAN PHYSICAL JOURNAL E

Regular Article

Hydrated cholesterol: Phospholipid domains probed by synchrotron radiation

I. Solomonov[1], J. Daillant[3,a], G. Fragneto[2], K. Kjaer[5], J.S. Micha[4], F. Rieutord[4], and L. Leiserowitz[1,b]

[1] Department of Materials and Interfaces, The Weizmann Institute of Science, Rehovot, 76100, Israel
[2] Institut Laue-Langevin, 6 Rue Jules Horowitz, BP 156, 38042 Grenoble Cedex 9, France
[3] CEA, IRAMIS, LIONS, CEA-Saclay, F-91191, Gif-sur-Yvette, France
[4] CEA-INAC, 17 Avenue des Martyrs, F-38054 Grenoble Cedex 9, France
[5] Niels Bohr Institute, University of Copenhagen, Universitetsparken 5, DK-2100 Copenhagen, Denmark

Received 21 January 2009 and Received in final form 12 May 2009

Abstract. X-ray scattering experiments on mixed films of cholesterol and phospholipids at air-water and Si solid-water interfaces were undertaken to glean information on pathological crystallization of cholesterol bilayers. Grazing-incidence X-ray diffraction patterns at the air-water interface of various cholesterol:dipalmitoyl-phosphatidylcholine (Ch:DPPC) monolayer mixtures compressed beyond monolayer collapse yielded the established $10 \times 7.5\,\text{Å}^2$ Ch bilayer motif, for Ch:DPPC molar ratios higher than 2.5:1. Attempts to obtain a diffraction signal from various Ch:phospholipid film mixtures at the Si solid-water interface, indicative of the presence of the Ch bilayer motif, were unsuccessful. Only after removal of sufficient water from the cell was a weak diffraction signal obtained suggestive of a cholesterol film two bilayers thick. Off-specular X-ray reflectivity measurements made on a 1.75:1 mixture of Ch and bovine cardiac phosphatidylcholine (BCPC) deposited as a bilayer on a Si wafer and placed in a cell filled with water yielded positive results. The derived electron density profile showed the presence of a bilayer mixture consistent with a phase separation of cholesterol and BCPC, and possible formation of a crystalline cholesterol bilayer within the hydrated mixed bilayer, but not a proof thereof.

PACS. 87.14.Cc Lipids – 87.16.dr Assembly and interactions – 87.16.dt Structure, static correlations, domains, and rafts – 87.64.Bx Electron, neutron and X-ray diffraction and scattering

1 Introduction

Cholesterol (Fig. 1), the most abundant sterol in animal tissues, is a component of cell membranes, plasma lipoproteins and a precursor in the biosynthesis of bile salts and hormones. Besides its role in controlling the mechanical properties of cell membranes, cholesterol, together with sphingolipids, forms organized domains, the so-called lipid rafts, which participate in distributing proteins to the cell surface, cell signal transduction and activation of immune responses. Abnormally high physiological levels of cholesterol may lead to its precipitation into crystallites that appear in atherosclerotic plaque [1,2], in gallstones [3] and in cataractous eye lenses [4].

Studies on cholesterol crystallization in model or native bile solutions by X-ray diffraction and more recently by cryo-transmission electron microscopy (cryo-TEM) describe the initial precipitation of early formed filamentous crystallites of cholesterol in bile solution of a previously unknown phase, followed by transformation to plates of the stable monohydrate form [5]. This crystallization process is similar to that observed in cultured foam cells insofar that the crystals appeared as needles, helices and plates [6].

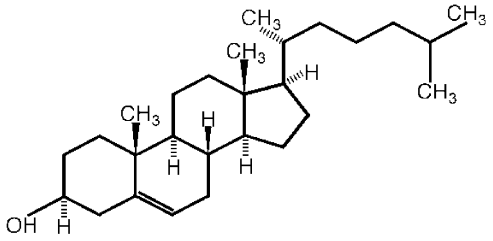

Fig. 1. Molecular structure of cholesterol.

Crystalline nucleation of cholesterol at the air-water interface has been studied by grazing-incidence X-ray diffraction (GIXD) using synchrotron radiation. The various stages of cholesterol molecular assembly, from

[a] e-mail: jean.daillant@cea.fr
[b] e-mail: leslie.leiserowitz@weizmann.ac.il

Published online: 23 July 2009

monolayer to three bilayers incorporating interleaving hydrogen-bonded water layers in a monoclinic cholesterol monohydrate phase, were monitored by GIXD and their structures characterized to near atomic resolution [7]. These cholesterol multilayers were generated by film compression beyond monolayer collapse, with the monolayer incorporating about 17% phospholipid. The monolayer structure was poorly ordered crystallizing in an arrangement of trigonal symmetry, as derived from the GIXD pattern [8], whereas the multilayers all incorporated the same bilayer motif possessing a monoclinic unit cell ($a = 10.2$ Å, $b = 7.6$ Å, $c = 68.2$ Å, $\alpha = \gamma = 90°$, $\beta = 95°$, space group $A2$). Partial compression of a pure cholesterol monolayer yielded a trilayer composed of an underlying crystalline $10 \times 7.5\,\text{Å}^2$ bilayer structure covered by a disordered cholesterol layer, that transformed with time into a trilayer [8] with a structure akin to that of the stable macroscopic triclinic monohydrate form ($a = 12.4$ Å, $b = 12.4$ Å, $c = 34.4$ Å, $\alpha = 92°$, $\beta = 98°$, $\gamma = 101°$, space group $P1$ [7]). High compression yielded a multilayer [7] of the thermodynamically stable triclinic monohydrate. Transformation from the metastable monoclinic monohydrate multilayer crystal to that of the stable triclinic form occurred via a single-crystal-to-single-crystal mechanism, at least in the early stages of the transition [7].

The metastable monoclinic phase has been shown [7] to be very similar to that of the metastable phase of cholesterol that first crystallizes from bile solution [5]. The preferred nucleation of the monoclinic phase of cholesterol monohydrate followed by transformation to the stable monohydrate structure has been qualitatively explained [7] in terms of the energetically more stable cholesterol layer arrangement of the former $10 \times 7.5\,\text{Å}^2$ motif (Fig. 2a), but a more favourable O-H···O hydrogen-bonding arrangement of the latter (Fig. 2d), involving the H_2O molecules and sterol OH groups. This comparison is elaborated upon in the legend of Figure 2.

Rothblat and coworkers [6] have proposed that the nucleation site of cholesterol in atherosclerotic plaques may occur within the biomembrane. Tulenko, Mason and coworkers have studied, by small-angle X-ray diffraction, the physical effects of cholesterol on arterial smooth muscle membranes isolated from control and cholesterol-fed atherosclerotic rabbits [9]. Their findings indicate that *in vivo* feeding of cholesterol causes cholesterol-phospholipid interactions in the membrane bilayer that alter the bilayer structure and organization. Their control experiments on reconstituted cardiac lipid bilayers show that beyond a saturated membrane cholesterol concentration in bovine cardiac phosphatidylcholine (BCPC), phase separation occurs, resulting in the formation of separate cholesterol crystalline domains when the cholesterol:phospholipid molar ratio is higher than 1:1.

For cholesterol to form the $10 \times 7.5\,\text{Å}^2$ bilayer in a biomembrane would require a sterol concentration large enough not only to phase-separate within each of the two biomembrane leaflets, but also bring about an interlayer overlap sufficient to generate the $10 \times 7.5\,\text{Å}^2$ bilayer motif, which might then act as a nucleating agent for extracellular cholesterol crystallization. Regarding the cholesterol

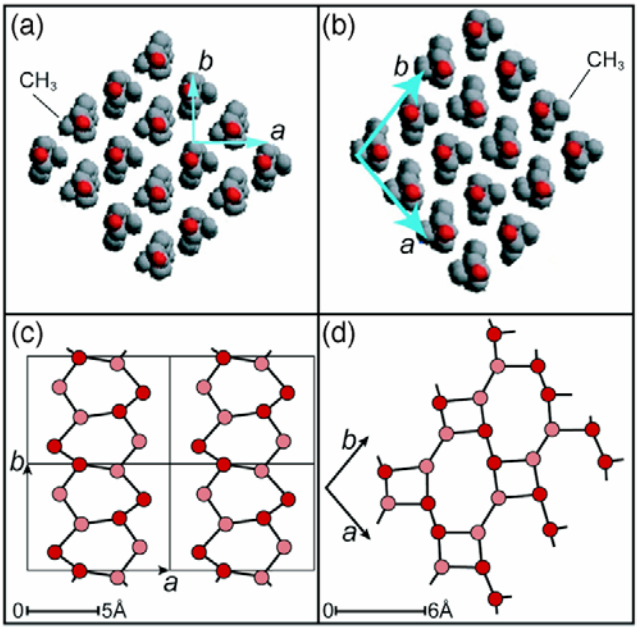

Fig. 2. (Colour on-line) Packing arrangements of the two crystalline polymorphs of cholesterol monohydrate. (a,b) Intralayer structures of the $10 \times 7.5\,\text{Å}^2$ and $12.4 \times 12.4\,\text{Å}^2$ cholesterol motifs, respectively, viewed down the long molecular axis. The axially oriented sterol methyl groups in each motif are denoted (see Fig. 1). The hydroxyl O atoms are coloured red. The $10 \times 7.5\,\text{Å}^2$ layer contains two cholesterol molecules per asymmetric unit, arranged such that the two axially oriented methyl groups per sterol (see Fig. 1) of neighbouring molecules interleave along the b-axis. By comparison, these methyl groups in the stable triclinic $12.4 \times 12.4\,\text{Å}^2$ motif point towards one another, suggesting a less stable arrangement. Independent evidence in favour of the greater stability of the $10 \times 7.5\,\text{Å}^2$ bilayer motif stems from the fact that of the 17 different three- and two-dimensional (*i.e.*, 3D and 2D) crystalline phases of cholesterol and its derivatives, listed in the Supplementary Material of [7], 15 phases embody the $10 \times 7.5\,\text{Å}^2$ unit cell. Therefore, the $12.4 \times 12.4\,\text{Å}^2$ bilayer motif is the exception. The H-bond arrangement interlinking the bilayers of the $12.4 \times 12.4\,\text{Å}^2$ motif (panel 2d) contains three H-bonds for each participating O atom; in the corresponding H-bonding motif of the $10 \times 7.5\,\text{Å}^2$ phase (panel 2c), only half the number of O atoms participate in three H-bonds, the remaining half form two H-bonds per O atom. The O atoms belonging to the sterol OH groups and the water H_2O molecules are coloured full red and light red, respectively.

domains within each leaflet, prior to the proposed crystalline bilayer formation, there is the question of the effect thereon by the lipids within each leaflet. For example, in a monolayer mixture of cholesterol with the diacyl C16 ceramide lipid on water [10], the latter is incorporated as solid solution up to concentrations of 33% into the 2D crystal domains of cholesterol.

Thus we undertook a study by GIXD and X-ray reflectivity (XR) of a synthetic cholesterol:phospholipid membrane floating in water next to a flat Si(111) surface, in order to try to obtain evidence in favour of the formation of the cholesterol $10 \times 7.5\,\text{Å}^2$ bilayer motif. Synthetic

phospholipid bilayers in bulk water next to a solid surface have been examined by various groups using specular and off-specular X-ray reflectivity probes [11–13], and more recently grazing-incidence X-ray diffraction [14,15].

As a preliminary step towards this aim, we first undertook a GIXD study of various cholesterol:dipalmitoylphosphatidylcholine (Ch:DPPC) monolayers on water compressed beyond their monolayer collapse point.

2 Materials and experimental methods

2.1 Materials

Cholesterol and 1,2 dipalmitoyl-*sn*-glycero-3-phosphatidylcholine (DPPC) of the highest purity available were obtained from Sigma. Bovine cardiac phosphatidylcholine (BCPC), with a fatty acid % distribution for n:m acyl chains (where n is the total number of C atoms and m the number of C=C bonds in the chain) of 23% 16:0; 1% 16:1; 6% 18:0; 13% 18:1; 43% 18:2; 1% 18:3; 6% 20:4 and 7% others, was purchased from Avanti Polar Lipids.

Lipid/chloroform solutions (*ca.* 0.1 mg/ml) were used to form the monolayer films at the air-water interface for surface pressure-molecular area isotherms and GIXD measurements.

2.2 Grazing-incidence X-ray diffraction at the air-water and water-solid interfaces

A detailed description of GIXD applied to films on liquid surfaces has been given elsewhere [16–18]. The GIXD experiments described here were performed on the liquid surface diffractometer at the undulator BW1 beam line at the HASYLAB synchrotron source, DESY. The films were spread on the water surface of a Langmuir trough in a homogeneous manner at room temperature. The air surrounding the trough was replaced by helium to reduce X-ray background scattering. The X-ray diffraction measurements were performed with the water subphase cooled to 5 °C. A monochromatic X-ray beam ($\lambda = 1.304$ Å) was adjusted to strike the liquid surface at an incident angle $\alpha_i < 0.85\alpha_c$, where α_c is the critical angle for total external reflection; this maximizes surface sensitivity. For GIXD on water, the signals are obtained from thin film crystallites randomly oriented about the water surface normal in the form of a 2D "powder". The size of the illuminated X-ray footprint on the liquid surface was 50 mm × 2 mm.

For the films on a solid support (see [13] for a detailed description of the experimental setup), a Teflon sample cell with thin ($\sim 50\,\mu$m) Teflon windows was filled with water and contained the silicon substrate. The cell was enclosed in a copper/aluminium box in which water was circulated at a controlled temperature. The first cholesterol:phospholipid layer was deposited on the substrate at room temperature from a monolayer spread from a 1 mg/ml solution in chloroform compressed at 35 mN/m surface pressure on the water surface by the classical

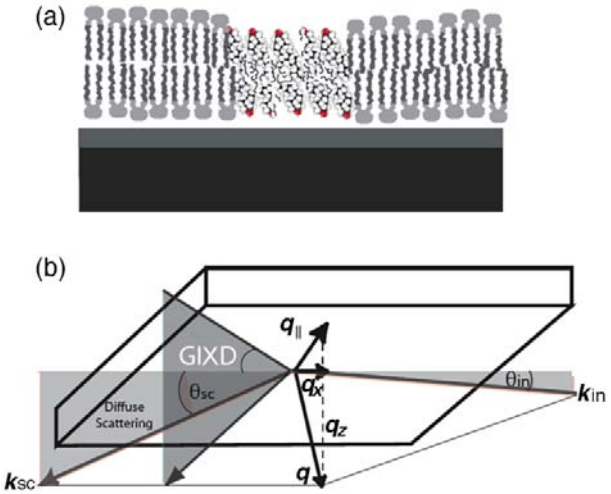

Fig. 3. Schematic of the sample. (a) A mixed phospholipid-cholesterol bilayer residing above a thick silicon substrate (black) and a nanometric silicon oxide (dark grey). The cholesterol and phospholipid domains in each leaflet are assumed to have phase-separated and make interlayer contacts with molecules of their own kind. (b) The geometry of the grazing-incidence X-ray diffraction and off-specular setup.

Langmuir-Blodgett (LB) technique (vertical sample transfer). The second layer was transferred by the Langmuir-Schaeffer technique (horizontal sample transfer) [19]. Samples were prepared using the Langmuir trough (NIMA, UK) available at the Institut Laue-Langevin. A schematic view of a bilayer composed of phase-separated phospholipid and cholesterol molecules, residing on the Si surface is depicted in Figure 3a.

The synchrotron radiation white beam produced by the bending magnet at the ESRF beam-line BM32_IF was first reflected by a platinum-coated, vertically focusing mirror. The energy was fixed by using a two-crystal Si(111) monochromator with sagittal (horizontal) focusing of the second crystal. The experiments were performed using 20 keV ($\lambda = 0.619$ Å) or 27 keV ($\lambda = 0.459$ Å) radiation, primarily the former, hard enough to penetrate the 25 mm of water in the cell, with roughly 38% transmission at 27 keV and 17% transmission at 20 keV. The grazing angle of incidence was fixed below the critical angle for total external reflection at the silicon-water interface. The dimensions of the X-ray footprint on the Si surface were $\sim 20\,\text{mm} \times 5\,\text{mm}$. A schematic view of the GIXD and off-specular reflectivity experimental setup is presented in Figure 3b.

2.3 Off-specular X-ray reflectivity measurements

For the off-specular reflectivity measurements the incident beam on the sample was limited by a 16-μm-high, 500-μm-wide slit, and its intensity was measured by using a photodiode monitor. For the off-specular measurements we fixed the grazing angle of incidence below θ_c, at $\theta_{\text{in}} = 10^{-3}$ rad and varied the detector angle, θ_{sc}. The temperature of the

cell was kept at roughly 7 °C. The electron density profile of the film was obtained from the diffuse reflectivity curve, following the method described in detail in [13] and reproduced briefly below.

Because scattering cross-sections are large in the total external reflection region, we must use a better approximation than the (kinematic) Born Approximation. Since our bilayers have only weak electron-density contrast with water, we can apply a perturbation theory (Distorted Wave Born Approximation) using as the reference state an ideally flat, substrate-water interface for which the scattering can be exactly calculated (Fresnel equations), and treating the bilayer as a weak perturbation. To lowest approximation, the scattering cross-section (power scattered per unit solid angle in the scattering direction, for a unit incident flux) is:

$$\mathrm{d}\sigma/\mathrm{d}\Omega \propto \left| \int \rho(z) \exp(iqz) \mathrm{d}z \right|^2 \exp(-{q_z}^2 \langle z \rangle^2) \times \int \mathrm{d}x \mathrm{d}y \left(\exp({q_z}^2 \langle z(0,0) z(x,y) \rangle) - 1 \right) \exp(iq_x x + q_y y), \quad (1)$$

where $\langle z \rangle^2$ is the film roughness and $\langle z(0,0)z(x,y) \rangle$ its height-height correlation function. For small enough q_z values, the exponentials can be expanded to lowest order, and we see that the last two terms in the equation reduce to the Fourier transform of the height-height correlation function, which is simply the roughness spectrum of the film. The scattering cross-section is therefore simply the roughness spectrum of the film times the Fourier tranform of the electron density profile along the film normal. This last term gives rise to the interferences visible in the scattered intensity. These interferences are similar to those obtained in reflectivity: they are interferences between beams reflected (in reflectivity) or scattered (in diffuse scattering) at large refractive index gradients. The electron density was obtained by expanding

$$\rho(z) - \rho_{\mathrm{water}} = F_0/D + \sum_1^{h_{\max}} F_h \cos(2\pi h z/D), \quad (2)$$

where D is the layer thickness. Fourier transforming, we have

$$\rho(z) = \sum_{-h_{\max}}^{h_{\max}} F_h \sin(qD/2 - \pi h)/(qD/2 - \pi h),$$

which can be inserted into equation (1) together with

$$\langle z(0)z(x) \rangle (k_B T/2\pi\sqrt{\Delta})[K_0(q_1 x) - K_0(q_2 x)],$$

where $\Delta = \gamma^2 - 4U_\kappa$, $q_1 = \sqrt{(\gamma - \Delta)/2\kappa}$, $q_2 = \sqrt{(\gamma + \Delta)/2\kappa}$, with K_0 the modified Bessel function of the second kind of order 0, U the second derivative of the interaction potential between the membrane and the substrate, γ the membrane tension and κ its rigidity. Fitting to the parameters yields the F_h which can then be used to reconstruct the electron density.

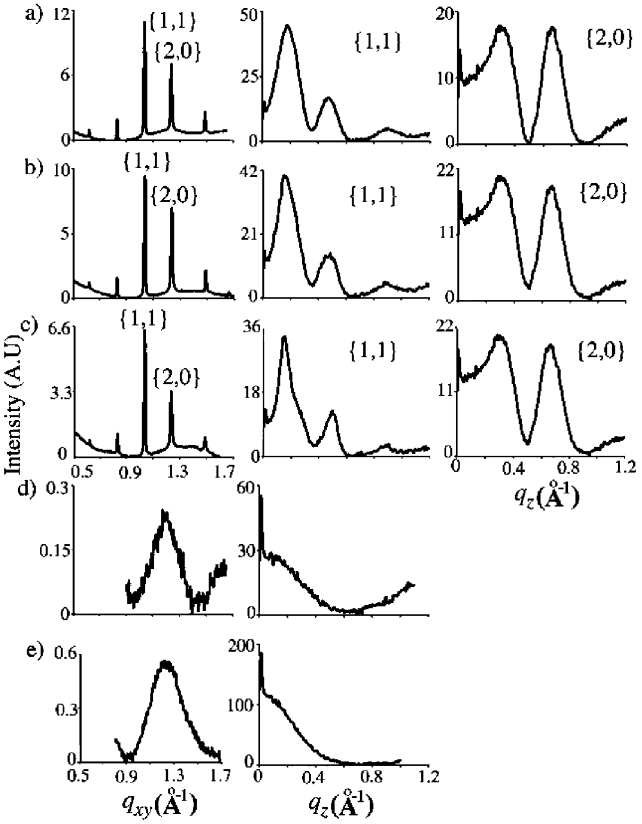

Fig. 4. GIXD patterns of compressed films of five Ch:DPPC mixtures at the air-water interface: (a) 5:1, (b) 2.5:1, (c) 2.25:1, (d) 2:1, (e) 1:1. Left column: the Bragg peak profiles $I(q_{xy})$. Center and right columns: corresponding Bragg rod intensity profiles $I(q_z)$. The $\{1,1\}$ and $\{2,0\}$ reflections of mixtures (a-c) are specified.

3 Results

3.1 Compressed films of cholesterol (Ch)-DPPC mixtures at the air-water interface

As mentioned above, in order to derive a rough initial measure of the tendency for crystalline multilayer formation of cholesterol (Ch) incorporating the $10 \times 7.5\,\text{Å}^2$ bilayer motif from various mixtures with phospholipid (DPPC), grazing-incidence X-ray diffraction data of Ch:DPPC mixtures, ranging from 5:1 to 1:1, were measured using the liquid surface diffractometer. The $10 \times 7.5\,\text{Å}^2$ bilayer is easily recognized by two Bragg rods $q(1,1) = 1.035\,\text{Å}^{-1}$ and $q(2,0) = 1.245\,\text{Å}^{-1}$ in its GIXD pattern [8]. The Ch:DPPC monolayer was compressed well beyond monolayer collapse to a nominal area-per-molecule of $17\,\text{Å}^2$, corresponding to crystalline bilayer formation of cholesterol [8] for the 5:1 Ch:DPPC mixture. The Ch:DPPC mixtures down to 2.25:1 yielded GIXD patterns (Fig. 4a-c) similar to that obtained for the 5:1 Ch:DPPC mixture. Below the 2.25:1 molar ratio, one broad Bragg reflection was observed (Fig. 4d,e, left), with a d spacing of 5.1 Å, as derived from the q_{xy} value of $1.22\,\text{Å}^{-1}$, the Bragg rod of which (Fig. 4d,e, right) peaks at $q_z = 0\,\text{Å}^{-1}$

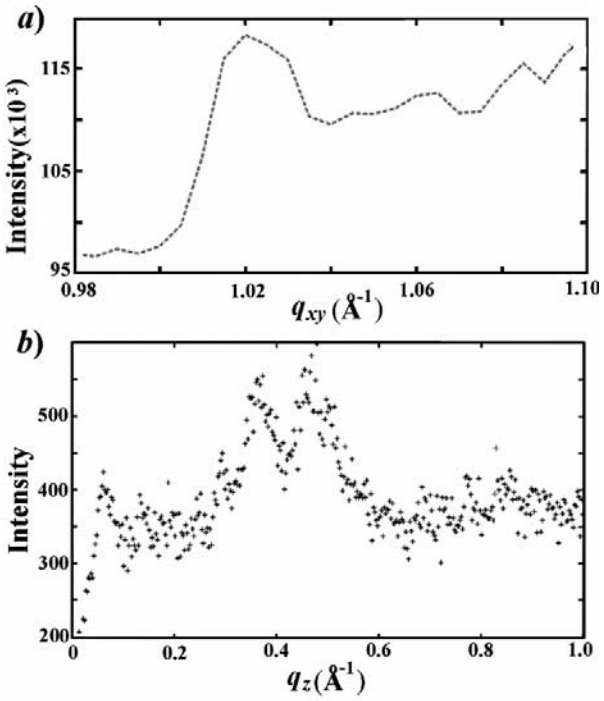

Fig. 5. GIXD pattern of the crystalline double bilayer of 5:1 Ch:DPPC mixture at the Si surface-air interface: (a) The Bragg peak profiles $I(q_{xy})$. (b) The Bragg rod intensity profile $I(q_z)$ at a q_{xy} value of 1.02 Å^{-1}.

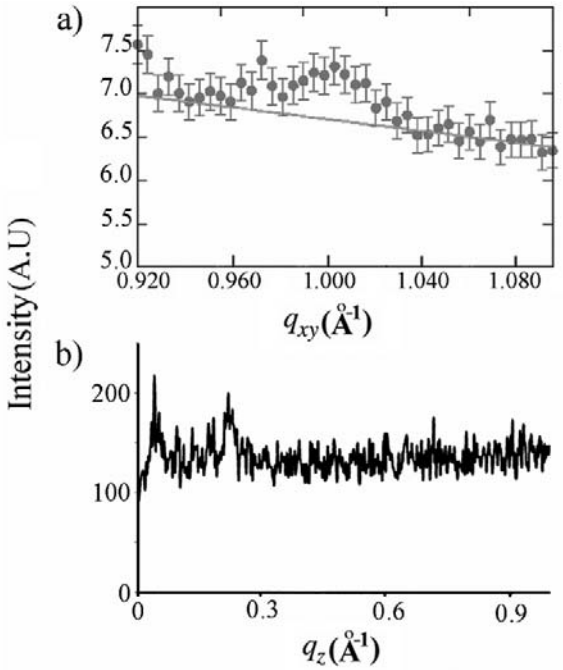

Fig. 6. GIXD pattern of the crystalline multilayer of 2.5:1 Ch:DPPC mixture at the Si surface-air interface: (a) The Bragg peak profiles $I(q_{xy})$. (b) The Bragg rod intensity profile $I(q_z)$ at a q_{xy} value of 1.0 Å^{-1}.

with a full width at half-maximum (FWHM) of $\Delta q_z = 0.28$ Å^{-1}. The Scherrer formula [20] then yields an estimate of the layer thickness $0.9 \times 2\pi/\Delta q_z = 20$ Å, which corresponds approximately to the length of the palmitoyl chain of DPPC. We interpret the broad Bragg peak with the d spacing of 5.1 Å to arise from a solid solution of cholesterol and DPPC, where the molecules are arranged in a manner akin to a 2:1 solid solution of cholesterol and ceramide [10].

3.2 Ch:phospholipid film mixtures at the Si solid-water interface

3.2.1 Measurement and analysis of GIXD data

For the Ch:DPPC and Ch:BCPC films prepared at the Si solid-water interface, we limited the search for evidence of formation of the 10×7.5 Å^2 bilayer to that of the $\{1,1\}$ Bragg rod ($q_{xy} = 1.035$ Å^{-1}), which is the strongest X-ray reflection in the GIXD patterns of a cholesterol bilayer on water (Fig. 4a-c). None of the Ch:DPPC and Ch:BCPC films adsorbed to the flat Si surface in water yielded unequivocal proof of the presence of the $\{1,1\}$ Bragg rod indicative of the cholesterol 10×7.5 Å^2 bilayer motif. Yet, when sufficient water was removed from the cell such that a potentially diffracting X-ray beam did not traverse the 25 mm of water in the cell, Bragg rods were observed for the two Ch:DPPC mixtures (5:1 and 2.5:1) that were examined (Figs. 5, 6). The Bragg rod of the 5:1 mixture, integrated along the vertical component q_z of the scattering vector q, plotted as a function of the horizontal component q_{xy}, (Fig. 5a), displays a maximum, in agreement with the GIXD pattern of the 10×7.5 Å^2 bilayer on water (Figs. 4a-c, left). The variation in intensity of the Bragg rod along the vector q_z, (Fig. 5b) at the Bragg peak intensity maximum, $q_{xy} = 1.02$ Å^{-1} in Figure 5a, differs from that of the $\{1,1\}$ rods shown in Figures 4a-c (right). The full width at half-maximum ($\Delta q_z = 0.08$ Å^{-1}) of the two Bragg rod intensity maxima along the intensity profile (Fig. 5b) yields a crystalline film of thickness $0.9 \times 2\pi/\Delta q_z = 70$ Å, which corresponds to two cholesterol bilayers. The separation in q_z of ~ 0.1 Å^{-1} between the two maxima is less than the corresponding value of ~ 0.3 Å^{-1} in Figure 4a-c (right), indicating a difference in structure. We may derive, but with less certainty, a similar conclusion from the GIXD results of the 2.5:1 mixture, the intensity profile along q_{xy} peaks at a value of 1.005 Å^{-1} (Fig. 6a), where the corresponding Bragg rod profile plotted along q_z (Fig. 6b) indicates a multilayer, according to the FWHM $\Delta q_z = 0.035$ Å^{-1} of the intensity profile maximum at $q_z = 0.22$ Å^{-1}.

3.2.2 Analysis of diffuse X-ray reflectivity data of 1.75:1 Ch:BCPC bilayer

As mentioned above, we could not address by GIXD the question of whether the cholesterol 10×7.5 Å^2 bilayer motif is adopted in a cholesterol-phospholipid bilayer at

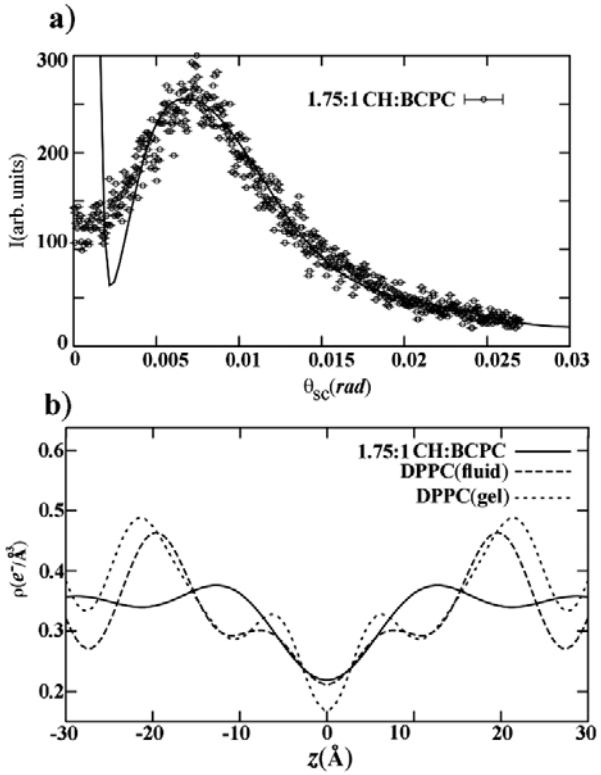

Fig. 7. (a) Diffuse X-ray reflectivity curve of 1.75:1 Ch:BCPC mixture at the Si surface-water interface. (b). Electron density profile of the bilayer of the 1.75:1 Ch:BCPC mixture at the Si surface-water interface as well as the electron density profiles of pure DPPC in fluid and gel phases.

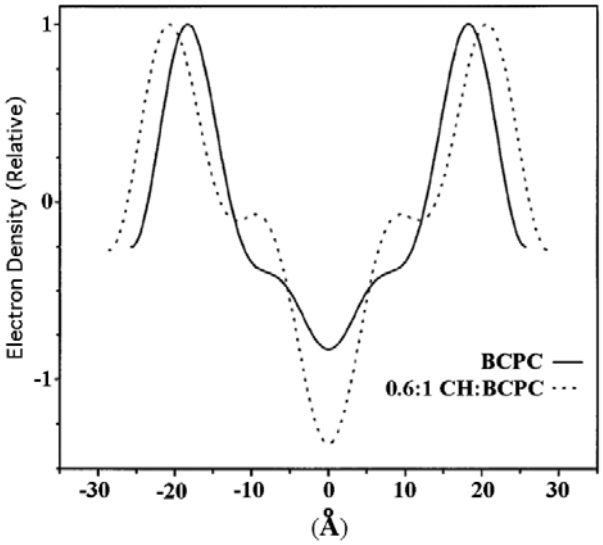

Fig. 8. Electron density profile of the bilayer of pure BCPC and of the 0.6:1 Ch:BCPC mixture obtained from low-angle X-ray diffraction Bragg reflections of reconstituted vesicular membrane multilayers.

the solid-water interface in the presence of excess water. Nevertheless, experimental evidence supporting this hypothesis for a cholesterol:phospholipid mixture with a molar ratio less than 2:1 may be obtained from diffuse X-ray reflectivity (DXR) measurements made on a 1.75:1 mixture of cholesterol (Ch) and bovine cardiac phosphatidylcholine (BCPC) deposited as a bilayer on a Si wafer, and placed in a cell filled with water.

The electron density profile was obtained from DXR measurements following the method described in Section 2. We note that the electron density profile is constrained to explicitly exhibit mirror symmetry, as expressed by equation (2), which should be qualitatively consistent with the actual bilayer structure. The electron density profile of 1.75:1 Ch:BCPC derived from the DXR curve (Fig. 7a) shows two inner and two outer maxima (Fig. 7b). The electron density distributions of a pure DPPC bilayer floating in water at a Si-water interface, derived from a DXR curve [13], are included for comparison. They also exhibit two inner and two outer maxima. The outer maxima originate from the maximum in the DXR curve (59–60 Å) and the inner maxima from the tail in the DXR curve, indicating that both the inner and outer maxima are real. We may rationalize the higher density of the inner maxima of the 1.75:1 Ch:BCPC mixture in terms of a higher concentration of cholesterol, which is more well packed and electron-rich than the corresponding double-acyl chain system of DPPC; the repeat area per molecule of cholesterol in the 10×7.5 Å^2 bilayer motif and of dimyristoyl-phosphatidylcholine (DMPC) in the bilayer of its reported 3D crystal structure [21] are the same (39 Å^2). We also note that the separation between the two inner maxima of 1.75:1 Ch:BCPC in Figure 7b is consistent with the 34 Å thickness of the cholesterol bilayer in the 10×7.5 Å^2 motif. The outer pair of maxima in the 1.75:1 Ch:BCPC bilayer are more widely separated and also have a lower electron density than the outer pair in pure DPPC (Fig. 7b), the maxima of which clearly correspond to its phosphatidylcholine head groups. We may rationalize the lower electron density of the outer peaks in the 1.75:1 Ch:BCPC bilayer (Fig. 7b) in terms of a lower phospholipid concentration as well as the variation in the aliphatic chain lengths of BCPC (see Sect. 2.1), absent in DPPC. The significant increase in intrabilayer phospholipid head group separation of 1.75:1 Ch:BCPC compared with pure DPPC (Fig. 7b) is, by and large, in agreement with a longer average chain length of BCPC than that of DPPC as well as with the electron density distributions of reconstituted vesicular membrane multilayers of 0:1 Ch:BCPC and 0.6:1 Ch:BCPC bilayer mixtures obtained from low-angle X-ray diffraction data reported by Tulenko, Mason and coworkers [9] (Fig. 8). Furthermore, the relatively higher electron density of the two inner maxima of 1.75:1 Ch:BCPC in Figure 7b, which we attribute to the cholesterol molecules, is consistent with the electron density distribution of both the 0:1 Ch:BCPC and 0.6:1 Ch:BCPC bilayer mixtures. Tulenko *et al.* interpreted the increase in intrabilayer phospholipid head group separation with increased cholesterol concentration in terms of a phase separation within the bilayer between the cholesterol and phospholipid molecules.

4 Discussion and concluding remarks

The GIXD patterns at the air-water interface of various cholesterol-dipalmitoyl-phosphatidylcholine (Ch-DPPC) monolayer mixtures, compressed beyond monolayer collapse, yielded the cholesterol $10 \times 7.5\,\text{Å}^2$ bilayer motif for Ch-DPPC molar ratios higher than 2.5:1. Attempts to obtain a diffraction signal from Ch-phospholipid film mixtures at the Si solid-water interface, unequivocally indicative of the presence of the $10 \times 7.5\,\text{Å}^2$ bilayer motif, were unsuccessful. Only after removal of sufficient water from the cell was a weak diffraction signal obtained suggestive of a cholesterol film two bilayers thick.

The off-specular X-ray reflectivity measurements made on a 1.75:1 mixture of cholesterol and bovine cardiac phosphatidylcholine (Ch:BCPC) deposited as a bilayer on a Si wafer, and placed in a cell filled with water yielded positive results. The derived electron density profile displayed the presence of a bilayer mixture consistent with possible formation of a crystalline cholesterol bilayer within the hydrated mixed bilayer, which would naturally involve a phase separation of cholesterol and BCPC, as has also been claimed by Tulenko *et al.* [9]. Thus we tend to the view that a random distribution of cholesterol molecules within each of the two leaflets and not forming a crystalline cholesterol bilayer, would yield an electron density profile somewhat different to that obtained.

A driving force for the existence of a crystalline cholesterol bilayer in the 1.75:1 CH:BCPC mixture would be the energetic advantage thereby afforded; the exocyclic moieties of cholesterol, being branched, flexible and with a cross-sectional area less than that of the sterol group ($\sim 37.5\,\text{Å}^2$), would make favourable interlayer contacts that could also lead to partial interleaving between the exocyclic groups. The role played by the interlayer contacts towards enhancing molecular order is highlighted by the highly crystalline nature of the cholesterol bilayer, when compared with that of the monolayer [8]; we note that in the crystalline monolayer of cholesterol the exocyclic moiety is disordered, presumably because it does not form sufficiently close intermolecular contacts.

The acyl chains in the 1.75:1 CH:BCPC bilayer mixture (see Sect. 2.1) cannot make favourable interlayer contacts with cholesterol molecules in a disordered bilayer for various reasons; the mismatch in their cross-sectional areas, and the different lengths of the acyl chains, with a relatively high proportion bent as a result of lipid unsaturation (see Sect. 2.1). The results are certainly in agreement with the neutron diffraction studies by Harroun *et al.* [22] on the depth of cholesterol in phosphatidylcholine (PC) bilayers with low amounts of acyl unsaturation (*i.e.* 16:0-18:1 PC; 18:1-18:1 PC; 18:0-20:4 PC), according to which the sterol was in the "upright" orientation and positioned with the hydroxyl group close to the membrane surface.

Regarding future work, the GIXD patterns recently reported from a DPPE bilayer on a quartz wafer in the presence of excess water, [14] and from hydrated ceramide and DPPC bilayers by keeping the samples humidified [15], suggest that it should be possible to resolve the question of the bilayer structure of cholesterol in its mixtures with phospholipids in hydrated bilayer mixtures.

We thank HASYLAB and ESRF for synchrotron beamtime and ILL for use of the facility for sample preparation. This work was supported by the Kimmelman Center at the Weizmann Institute of Science.

References

1. D.M. Small, G.G. Shipley, Science **185**, 222 (1974).
2. D.M. Small, Arteriosclerosis **8**, 103 (1998).
3. H. Bogren, K. Larsen, Biochim. Biophys. Acta **75**, 65 (1963).
4. R.F. Jacob, R.J. Cenedella, R.P. Mason, J. Biol. Chem. **276**, 13573 (2001).
5. F.M. Konikoff, D.S. Chung, J.M. Donovan, D.M. Small, M.C. Carey, J. Clin. Invest. **90**, 1155 (1992).
6. G. Kellner-Welbel, P.G. Yancey, W.G. Jerome, T. Walser, R.P. Mason, M.C. Phillipis, G.H. Rothblatt, Arterioscler. Thromb. Vasc. Biol. **19**, 1891 (1999).
7. I. Solomonov, M.J. Weygand, K. Kjaer, H. Rapaport, L. Leiserowitz, Biophys. J. **88**, 1809 (2005).
8. H. Rapaport, I. Kuzmenko, S. Lafont, K. Kjaer, P.B. Howes, J. Als-Nielsen, M. Lahav, L. Leiserowitz, Biophys. J. **81**, 2729 (2001).
9. T. Tulenko, M. Chen, P.F. Mason, R.P. Mason, J. Lipid. Res. **39**, 947 (1998).
10. L. Scheffer, I. Solomonov, M.J. Weygand, K. Kjaer, L. Leiserowitz, L. Addadi, Biophys. J. **88**, 3381 (2005).
11. M. Vogel, C. Munster, W. Fenzl, T. Salditt, Phys. Rev. Lett. **84**, 390 (2000).
12. C.E. Miller, J. Majewski, T. Gog, T.L. Kuhl, Phys. Rev. Lett. **94**, 238104 (2005).
13. J. Daillant, E. Bellet-Amalric, A. Braslau, T. Charitat, G. Fragneto, F. Graner, S. Mora, F. Rieutord, B. Stidder, Proc. Natl. Acad. Sci. U.S.A. **102**, 11639 (2005).
14. C.E. Miller, J. Majewski, E.B. Watkins, D.J. Mulder, T. Gog, T.L. Kuhl, Phys. Rev. Lett. **100**, 058103 (2008).
15. R. Ziblat, K. Kjaer, L. Leiserowitz, L. Addadi, submitted for publication (2009).
16. J. Als-Nielsen, K. Kjaer, in *Phase Transitions in Soft Condensed Matter*, Vol. **211**, Series B, edited by T. Riste, D. Sherrington (Plenum Press, New York, 1989), p. 113.
17. I. Kuzmenko, H. Rapaport, K. Kjaer, J. Als-Nielsen, I. Weissbuch, M. Lahav, L. Leiserowitz, Chem. Rev. **101**, 1659 (2001).
18. T.R. Jensen, K. Kjær, in *Studies in Interface Science*, edited by D. Möbius, R. Miller (Elsevier, Amsterdam, 2001), p. 205.
19. L.K. Tamm, H.M. McConnell, Biophys J. **47**, 105 (1985).
20. A. Guinier, *X-ray Diffraction in Crystals, Imperfect Crystals, and Amorphous Bodies*, Section 5.5 (W.H. Freeman, San Francisco, 1963), p. 142.
21. H. Hauser, I. Pascher, R.H. Pearson, S. Sundell, Biochim. Biophys. Acta **650**, 21 (1981).
22. T.A. Harroun, J. Katsaras, S. Wassall, Biochemistry **45**, 1227 (2006).